Check for updates

The intramolecular hydrogen bonded–halogen bond: a new strategy for preorganization and enhanced binding†

Asia Marie S. Riel,‡ Daniel A. Decato,‡ Jiyu Sun, Casey J. Massena, Morly J. Jessop and Orion B. Berryman [ID] *

Natural and synthetic molecules use weak noncovalent forces to preorganize structure and enable remarkable function. Herein, we introduce the intramolecular hydrogen bonded–halogen bond (HB–XB) as a novel method to preorganize halogen bonding (XBing) molecules, while generating a polarization-enhanced XB. Positioning a fluoroaniline between two iodopyridinium XB donors engendered intramolecular hydrogen bonding (HBing) to the electron-rich belt of both XB donors. NMR solution studies established the efficacy of the HB-XB. The receptor with HB–XBs (**G2XB**) displayed a nearly 9-fold increase in halide binding over control receptors. Gas-phase density functional theory conformational analysis indicated that the amine stabilizes the bidentate conformation. Furthermore, gas-phase interaction energies showed that the bidentate HB–XBs of **G2XBme^{2+}** are more than 3.2 kcal mol^{-1} stronger than the XBs in a control without the intramolecular HB. Additionally, crystal structures confirm that HB–XBs form tighter contacts with I$^-$ and Br$^-$ and produce receptors that are more planar. Collectively the results establish the intramolecular HB–XB as a tractable strategy to preorganize XB molecules and regulate XB strength.

Introduction

Preorganization is a central tenet of supramolecular chemistry that facilitates precise molecular function and higher order self-assembly.[1–3] § Preorganized biomolecular structures rely on noncovalent interactions for their critical role in natural processes (*e.g.* catalysis, ion channels, signaling, nutrient transport, and antibodies). For example, the exceptional catalytic activity of phosphatase is aided by the secondary and tertiary structure imparted by noncovalent interactions. The rate of phosphate hydrolysis is enhanced by 10^{21} over the uncatalyzed reaction.[4] Nature's proficiency continues to inspire synthetic studies "beyond the molecule," as principles governing protein–ligand and protein–protein interactions are the same in synthetic systems.[5–9] Thus, developing new preorganization methods is valuable to all fields impacted by supramolecular chemistry. In this article, we introduce a novel strategy to preorganize structure and enhance halogen bonding (XBing)—the hydrogen bonded-halogen bond (HB–XB).

Preorganization of small molecules has largely focused on macrocycles since the seminal cation binding reports of Cram, Lehn, and Pedersen.[1,2,10–13] More recently, preorganized macrocycles,[14–18] rotaxanes,[19,20] and catenanes[21] have also successfully sequestered anionic and neutral guests. The utility of macrocyclization is unmistakable, yet synthetic challenges have encouraged the development of acyclic molecules that are preorganized by noncovalent interactions (*e.g.* hydrogen bonding,[22–27] steric effects,[28,29] ion-pairing,[30,31] and π-π stacking[32–34]). In particular, intramolecular hydrogen bonds (HBs) have been effective at preorganizing structure, including helicies,[35,36] cavitands[37–39] and ion transporters.[40] Internal[41] and external[22,26] intramolecular HBing are the two predominate strategies used for HB preorganization.[42] Internal intramolecular HBs (proximal to the binding site) usually share the HB donor between the receptor and the guest, which typically weakens the HB interaction to the guest. Alternatively, external intramolecular HBs (away from the binding site) can compete with the guest binding to the desired location. In contrast, the unique characteristics of a XB donor provides an opportunity for internal intramolecular HB preorganization that also enhances binding.

The XB—an attractive and highly directional noncovalent interaction between a polarizable electron-deficient halogen and an electron rich Lewis base[43]—is finding diverse applications in chemistry[44–46] and biochemistry.[47,48] The strict linearity of the XB arises from electronic anisotropy of the halogen donor. Polarization produces a partial positive σ-hole at the

University of Montana, 32 Campus Drive, Missoula, MT, USA. E-mail: orion. berryman@umontana.edu

distal end of the atom and an electron-rich region circling the halogen.[49] ¶ ‖ XB directionality has been exploited in selective anion binding,[44,50] organocatalysis,[29,51,52] crystal engineering,[53–55] and self-assembly.[56–59] Considering the required linear directionality of the XB interaction, XB based molecules should benefit more from preorganization than other less directional interactions. However, few XB receptors are non-covalently preorganized (Fig. 1).[29,60–63] **

Polarization-enhanced hydrogen bonding—where the heteroatom of a HB donor concurrently accepts a HB—is an established method to strengthen HBs.[64,65] However, despite many studies comparing the XB and HB, few have evaluated how they influence each other. Simultaneous XBing and HBing to a single Lewis base has been the primary focus, with evaluations in the gas, solution, and solid phases. Collectively the diverse findings—including both competitive and cooperative effects, geometric and energetic orthogonality, and unique anion binding selectivity—necessitate further study.[66–74] Studies evaluating the direct influences on each other—electron-rich belt of a XB donor or XBing to an electronegative region of a HB donor heteroatom—have been largely limited to intermolecular structural database and computational evaluations.[75,76] †† Computational reports of intermolecular HBing to XB donors suggest that HBs can have both cooperative and non-coooperative effects on XB strength.[66,77–86] More recently, a computational and protein data bank analysis found that ligand binding is improved by up to 250-fold when XB donors on the ligand accept HBs from the protein.[87] Remarkably, solution studies of HBing to XB donors are nonexistent.‡‡ Herein, we introduce a polarization-enhanced XB. Findings suggest that the intramolecular HB–XB can be used to non-covalently preorganize a molecule while simultaneously enhancing the XB interaction in solution, solid, and *in silico*.

Results and discussion

Design and synthesis of 1,3-bis(4-ethynylpyridinium) receptors

Recently our lab developed a bisethynyl receptor that binds anions and neutral Lewis bases with two iodopyridinium XB donors.[88,89] The alkynes promote rigidity and directionality, but their low rotational barrier allows the receptors to adopt three planar binding conformations (Fig. 2). Our interest in bidentate XB interactions prompted us to preorganize the receptor.

Fig. 2 ChemDraw representations of the three planar conformations obtained by rotating about the alkyne bonds: the bidentate conformation (left), where both XB donors are convergent; the S conformation (middle), where the XB donors are on opposite sides of the molecule; and the W conformation (right), where both XBs are directed away from the amine.

Macrocyclization and external intramolecular HBing (away from the binding site) were not synthetically tractable. However, we hypothesized that preorganization could be accomplished by HBing to the electron-rich belt of the XB donors with an electron-deficient aniline (Fig. 1d). The fluorinated core was introduced to increase the HB strength of the $-NH_2$ as halogens are regarded as poor acceptors. Initially, we pursued a tri-fluorinated derivative but synthetic difficulties prevented this possibility. We refer to these second-generation receptors as **G2XB** and **G2HB** (Scheme 1).

The synthesis of **G2XB**, **G2HB** and **G2XBme** is outlined in Scheme 1. 2,6-bis(ethynyl)-4-fluoroaniline (**2**) was synthesized by Sonogashira[90] cross-coupling 2,6-dibromo-4-fluoroaniline with trimethylsilylacetylene followed by removal of the trimethylsilyl protecting groups. Precursors **3** and **5** were synthesized by Sonogashira cross coupling **2** at the iodo-functionality of 3-bromo-4-iodopyridine or 4-iodopyridine, respectively. The XB donor iodines of **4** were installed by microwave assisted halogen exchange of **3**. Alkylation of the pyridines with octyl triflate activated the XB and HB donors of **4** and **5** respectively and enabled organic solubility. Anion metathesis of the triflate (OTf$^-$) counteranions for noncoordinating tetrakis (3,5-bis(trifluoromethyl)phenyl)borate (BAr^{F-})[91] anions produced **G2XB** and **G2HB** (see ESI†). The methyl derivative, **G2XBme**, was similarly synthesized for X-ray diffraction studies. **G1XB**, **G1HB** and **G1XBme** were synthesized as previously reported.[88]

Solution assessment of HB–XB preorganization and enhanced XB

^{1}H NMR titrations were conducted to probe intramolecular HB–XB preorganization and XB enhancement in **G2XB** (Table 1).
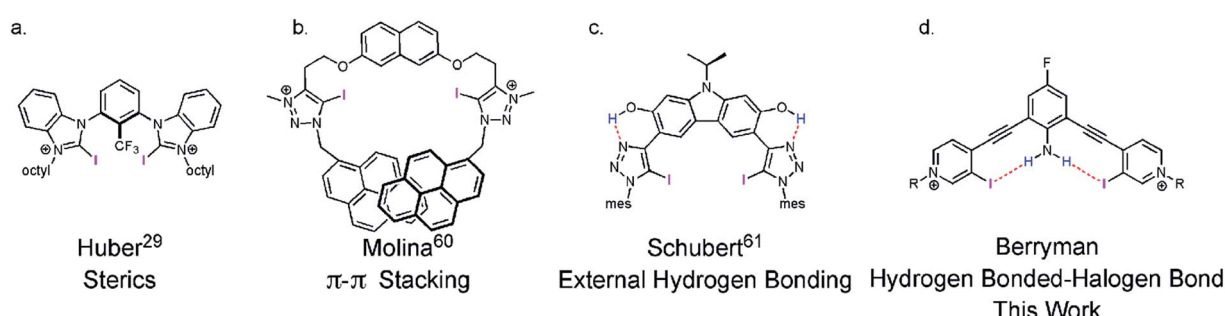
Fig. 1 Representative noncovalent preorganization strategies for XB receptors.
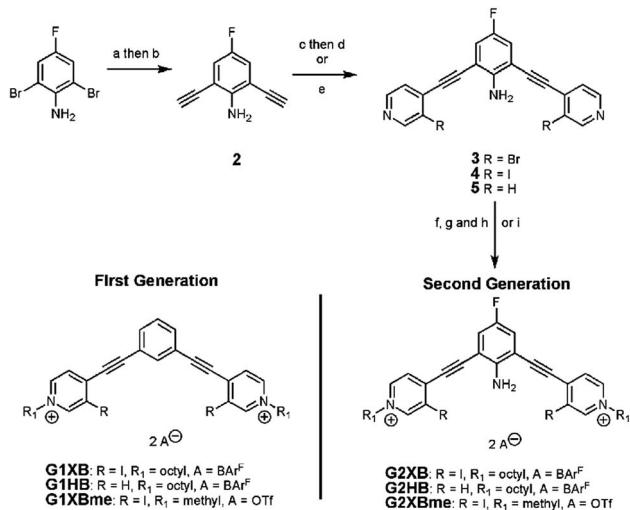
Scheme 1 Synthesis of **G2XB**, **G2HB** and **G2XBme** receptors. Reagents and conditions: (a) TMS-acetylene, Pd(PPh₃)₂Cl₂, Cu(I)I, DIPEA, DMF, overnight, N₂, 60 °C, 90%; (b) K₂CO₃, MeOH/DCM (1 : 1 v/v), 4 hours, rt, 73%; (c) 3-bromo-4-iodopyridine, Pd(PPh₃)₂Cl₂, Cu(I)I, DIPEA, DMF, overnight, N₂, rt, 90%; (d) NaI, Cu(I)I, 1,4-dioxane, *trans*-*N*,*N*′-dimethylcyclohexane-1,2-diamine, microwave reactor, 150 °C, 5.5 hours, 81%; (e) 4-iodopyridine, Pd(PPh₃)₂Cl₂, Cu(I)I, DIPEA, DMF, overnight, N₂, 60 °C, 58%; (f) octyl triflate, DCM, rt, overnight, 54%; (g) TBA⁺Cl⁻, MeCN, overnight, 77%; (h) Na⁺BArᶠ⁻, DCM, rt, overnight, 63%; (i) methyl triflate, DCM, rt, overnight, 89%.

Association constants were determined by HypNMR 2008[92] for each receptor and the tetra-*n*-butylammonium (TBA⁺) halides (Cl⁻, Br⁻ and I⁻). All titrations were performed in 60% CD₃NO₂/40% CDCl₃ at 25 °C to ensure solubility and to prevent the binding constants from exceeding the limit of NMR. Both XB receptors, **G2XB** and **G1XB**, exhibit anion-induced upfield pyridinium proton shifts, characteristic of XBing in solution.[93] In contrast, the pyridinium protons of the HB receptors, **G2HB** and **G1HB**, only shifted downfield, consistent with HBing in solution (see ESI†).

Intramolecular HB–XBs enhance halide binding by nearly 9-fold over **G1XB**, which lacks intramolecular HB–XBs. The halide K_{11} values for **G2XB** are 23 700 M⁻¹ for Cl⁻, 32 900 M⁻¹ for Br⁻ and 36 900 M⁻¹ for I⁻. In contrast, **G1XB** binds halides much more weakly with K_{11} values of 2630 M⁻¹ for Cl⁻, 4690 M⁻¹ for Br⁻, and 4380 M⁻¹ for I⁻. Additionally, both **G2XB** and **G1XB**

prefer larger halides (I⁻ ≈ Br⁻ > Cl⁻) which could be attributed to the size selective binding pocket and HSAB complementarity of the XB.[89,94] The second binding event (K_{12}) is quite weak for all receptors and likely represents nonspecific ion pairing to balance the charge.

To verify that the amine forms intramolecular HBs instead of HBing directly with the anions, the binding of **G2XB** was compared with three control receptors. **G2XB** binds halides more than an order of magnitude greater than **G2HB**, which contains the amine but lacks XB donors. The K_{11} values for **G2HB** are 2500 M⁻¹ for Cl⁻, 2110 M⁻¹ for Br⁻, and 1750 M⁻¹ for I⁻. Furthermore, the amine of **G2HB** marginally increases binding for both Br⁻ and I⁻ and even decreases Cl⁻ binding when compared to **G1HB**, which lacks both the amine and fluorine (**G1HB** K_{11} values of 9040 for Cl⁻, 1150 for Br⁻, and 1030 M⁻¹ for I⁻). Thus, the amine does not significantly HB to the halides in this system.

Comparing the binding of **G2HB** to **G1XB** establishes that the XB is more effective at binding Br⁻ and I⁻ than the HBs in **G2HB**. The K_{11} values of **G1XB** (4690 M⁻¹ for Br⁻ and 4380 M⁻¹ for I⁻) are more than double the K_{11} values of **G2HB** (2110 M⁻¹ for Br⁻ and 1750 M⁻¹ for I⁻). Collectively these studies support that intramolecular HB–XBs preorganizes the receptor and significantly enhances halide binding.

NMR analysis of chemical shifts, hydrogen/deuterium (H/D) exchange rates, and rotational barriers can provide solution evidence of intramolecular HBs to strong acceptors.[95,96] §§ In contrast, there is a deficiency of NMR studies on HBing to weak organic halogen acceptors.[97] Chemical shift analysis and H/D exchange experiments on this system support that intramolecular HBing occurs in **G2XB**. The NH₂ ¹H NMR resonance in **G2XB** was shifted downfield by 0.52 ppm (5.30 ppm, CDCl₃) as compared to **G2HB** (4.78 ppm, CDCl₃). The downfield resonance in **G2XB** is indicitive of deshielded protons which suggest that intramolecular HBing is occuring. H/D exchange experiments were conducted on **G2XB** and **G2HB**. **G2XB** had a slower H/D exchange than **G2HB**, which is attributed to intermolecular HBing and increased steric interactions in **G2XB** (see ESI†)[98,99] Additionally, variable temperature (VT) ¹H NMR was used to evaluate intramolecular HBing. Upon warming, the NH₂ signals for both **G2XB** and **G2HB** shift upfield.[35,36] ¶¶ However, the shift in **G2XB** is slightly more upfield (see ESI†), consistent with intramolecular HBing. Together, the solution studies

Table 1 Association constants for **G2XB**, **G2HB**, **G1XB** and **G1HB** with halides[a]

	G2XB		G1XB		G2HB		G1HB	
	K_{11} (M⁻¹)	K_{12} (M⁻¹)	K_{11} (M⁻¹)	K_{12} (M⁻¹)	K_{11} (M⁻¹)	K_{12} (M⁻¹)	K_{11} (M⁻¹)	K_{12} (M⁻¹)
Cl⁻	23 700	25	2630	37	2500	47	9040	38
Br⁻	32 900	35	4690	32	2110	44	1150	38
I⁻	36 900	28	4380	28	1750	44	1030	33

[a] The K_{11} and K_{12} values are reported as the average of three titration experiments. All titrations were performed in 40% CDCl₃/60% CD₃NO₂; errors are estimated at 10%. Tetra-*n*-butylammonium halides were used and titrations were performed at 25 °C. HypNMR 2008 was used to fit changes in chemical shift to a stepwise 1 : 1 and a 1 : 2 host-guest binding model. Continuous refinements of multiple isotherms provided stability constants (K_a) for all host-guest complexes in solution.

W Conformation   S Conformation   Bidentate

—   −0.68 kcal/mol   −1.29 kcal/mol
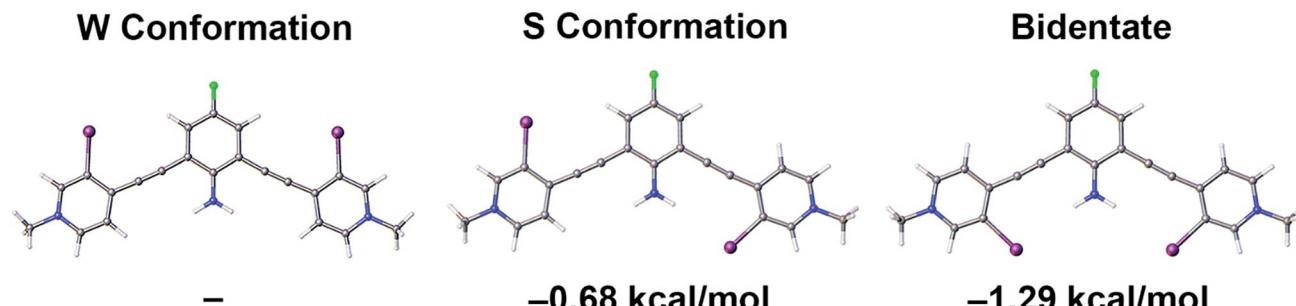
Fig. 3 Gas-phase DFT single point energy calculations of the three planar conformations of **G2XBme²⁺** highlight intramolecular HB–XB stabilization. Ball and stick models were produced from lowest energy conformations.

demonstrate that intramolecular HB-XB preorganization is operable and contributes to the improved halide recognition.

Computational evaluations of receptor conformations and XB enhancement

Gas-phase density functional theory (DFT) calculations further quantified the role of intramolecular HB–XBing in pre-organization and XB augmentation. To simplify calculations, three planar conformations of **G2XBme²⁺** were evaluated. Calculations were performed with the B3LYP functional ‖‖ using the Gaussian 09 suite of programs.[100] The 6-31+G (d,p) basis set was employed for all atoms except nitrogen and iodine. To appropriately account for the HB donor the aug-*cc*-pVTZ basis set was used for nitrogen.[101] To model the polarizable iodine the LANL2DZdp and effective core potential (ECP) was used.[102] The LANL2DZdp ECP basis set was downloaded from the EMSL Basis Set Exchange.[103] Crystal structures were used as starting positions for all calculations. Optimized geometries and frequencies were calculated to confirm molecules were at local minima (details in ESI†).

Single point energy calculations of **G2XBme²⁺** illustrate that intramolecular HB–XBs stabilize the receptor (Fig. 3). The number of intramolecular HB–XBs directly correlates with

receptor stability. The bidentate conformation, with two intra-molecular HBs, is more stable than the W conformation (no HB–XB) by 1.29 kcal mol⁻¹. The S conformation, with one intramolecular HB contact, is less stable than the bidentate conformation by 0.61 kcal mol⁻¹. The W conformation, lacking intramolecular HB–XBs, is the least stable and is 0.68 kcal mol⁻¹ higher in energy than the S conformation.

To further analyze how intramolecular HBs stabilize **G2XB**, conformational analysis about the alkynes of **G2XBme²⁺** and **G1XBme²⁺** were examined. **G2XBme²⁺** favors the bidentate conformation over the S conformer by over 0.60 kcal mol⁻¹ which is comparable to the single point energy calculations. In contrast, **G1XBme²⁺** favors the S conformer by 0.16 kcal mol⁻¹ over the bidentate conformation, highlighting the critical proximity of the HBing amine (see ESI†). Notably, addition of the intramolecular HBs increases the rotational barrier between the bidentate and S conformation by 1.64 kcal mol⁻¹. Both single point energy and alkyne conformational driving studies further support the hypothesis that HB–XB preorganizes bidentate XB conformations of **G2XB**.

Computations were also used to model how the intra-molecular HB influences the strength of the XB. The effect is illustrated by electrostatic potential (ESP) maps of **G1XBme²⁺**,
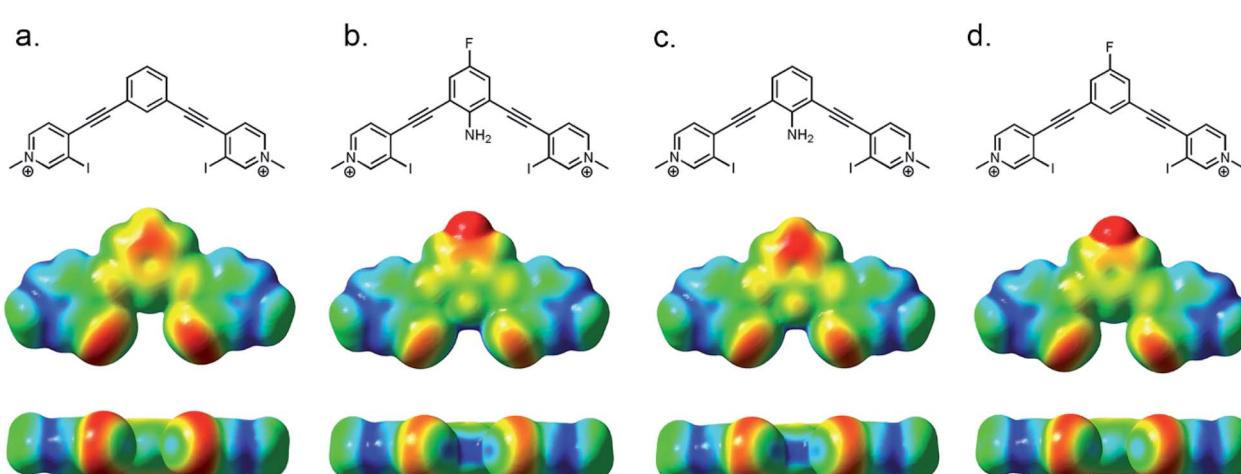
Fig. 4 ChemDraw and ESP maps of **G1XBme²⁺** (a), **G2XBme²⁺** (b), **G2XBme²⁺** with no fluorine (c) and **G2XBme²⁺** with no amine (d). All ESP maps are displayed on the same scale. Electron-deficient regions are blue and electron-rich regions are red.
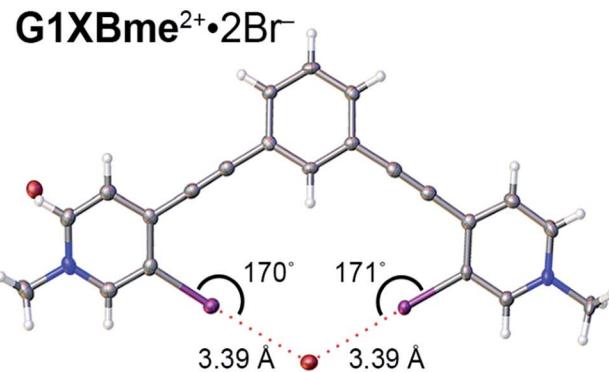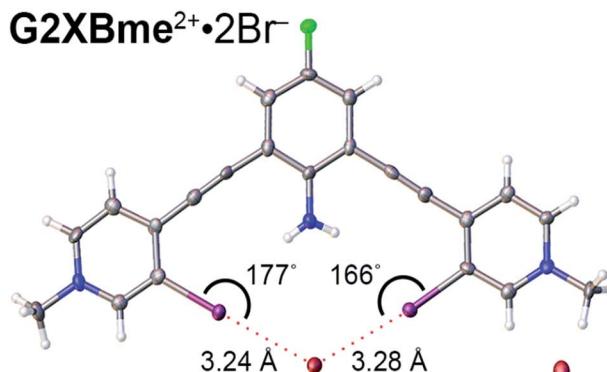
Fig. 5 Bidentate XBing conformations of **G2XBme²⁺·2Br⁻** (left) and **G1XBme²⁺·2Br⁻** (right). XB distances and angles are displayed. Thermal ellipsoids are drawn at the 50% probability level. **G1XBme²⁺·2Br⁻** crystallized with a methanol molecule which HBs with noncoordinating Br⁻ and is omitted for clarity.

G2XBme²⁺, and two derivatives of **G2XBme²⁺** (Fig. 4). **G2XBme²⁺** (Fig. 4b) has a larger, more electrophilic region at the σ-hole than **G1XBme²⁺** (Fig. 4a). This augmentation is attributed to the additional polarization by the intramolecular HB. The HB further polarizes the electron density around the halogen which strengthens the XB interaction. *** Additional calculations verify that the fluorine atom is not the cause of this effect. The derivative of **G2XBme²⁺** without the fluorine (Fig. 4c) has a similar σ-hole to **G2XBme²⁺**. However, when the amine is removed but the fluorine is retained, the σ-hole is markedly reduced (Fig. 4d).

The magnitude by which HBing enhances bidentate XBing in this system was evaluated by computing gas-phase interaction energies with Br⁻. The interaction energy is computed as the difference between the complex and the isolated consituents in the same geometry as the complex (see ESI†). **G2XBme²⁺** and the derivative of **G2XBme²⁺** with no amine (no HB–XBs), were compared. The presence of the amine in **G2XBme²⁺** strengthened the bidentate XB interaction by more than 3.23 kcal mol⁻¹ over the receptor with no HB–XB. Together, these calculations corroborate the solution data and the dual role of the HB–XB to enhance the σ-hole and promote preorganization.

HB–XB impact on solid-state features

The intramolecular HB–XBs in **G2XBme²⁺** promote the bidentate conformation. In contrast, previous solid-state studies of

G1XBme²⁺ produced structures with multiple conformations. Here, we present crystal structures of **G2XBme²⁺**, **G2XB²⁺**, and **G1XBme²⁺** that illustrate intramolecular HB–XBs facilitate planar conformations with stronger XB contacts for anion recognition. The receptors crystallize in the bidentate conformation with every halide, allowing direct comparison of the XB contacts and geometries of each receptor (crystal growth conditions and details in ESI†).

Bidentate XB structures

Both **G2XBme²⁺** and **G1XBme²⁺** crystallized with Br⁻ (Fig. 5) forming bidentate XB interactions with one Br⁻. As designed, **G2XBme²⁺** forms intramolecular HBs that influence both the receptor conformation and the strength of the XB. The intramolecular HBs in **G2XBme²⁺·2Br⁻** have N–H···I distances and angles of 2.96 (10) Å, 165 (6)° and 3.14 (14) Å, 155 (5)° that correlate well with a CSD search. ††† The amine protons preorganize the complex of **G2XBme²⁺·2Br⁻** resulting in pyridnium rings that twist out of coplanarity with the fluoroaniline core by only 4.8 (2) and 7.8 (2)°. In contrast, **G1XBme²⁺·2Br⁻** which lacks intramolecular HBs, is more distorted, with the pyridinium rings twisting out of coplanarity with the benzene core by 15.18 (12) and 14.13 (12)°. Additionally, the intramolecular HBs strengthen the XB. The XB distances and angles in **G2XBme²⁺·2Br⁻** are shorter and more linear with values of 3.2358 (11) Å, 176.86 (19)° and 3.2787 (11) Å, 166.78 (19)° (R_{IBr}
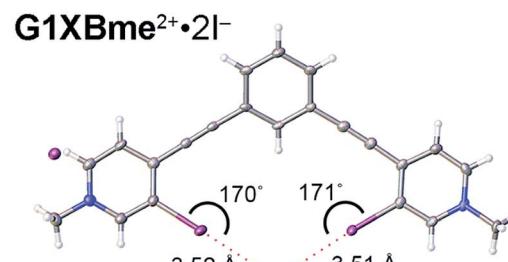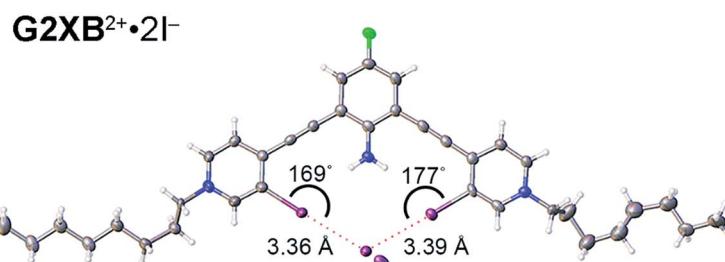
Fig. 6 Bidentate XB conformations of **G2XB²⁺·2I⁻** (left) and **G1XBme²⁺·2I⁻** (right). XB distances and angles are displayed. Thermal ellipsoids are drawn at the 50% probability level. **G1XBme²⁺·2I⁻** crystallized with a methanol molecule which exhibits HBing with noncoordinating I⁻ and is omitted for clarity.
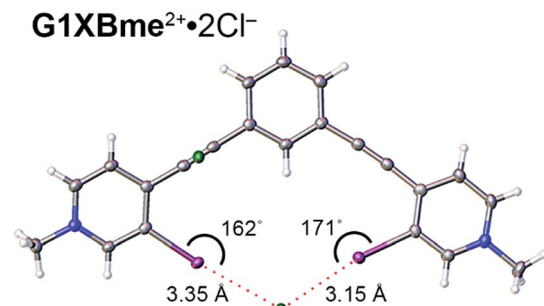
Fig. 7 Bidentate binding conformation of **G1XBme^{2+}·2Cl$^-$**. XB distances and angles are displayed. Thermal ellipsoids are drawn at the 50% probability level.

values of 0.82 and 0.83). The distances and angles of **G1XBme^{2+}·2Br$^-$** are longer at 3.3938 (5) Å, 169.9 (1)° and 3.3905 (5) Å, 171.13 (10)° (R_{IBr} values of 0.87 and 0.87). The second Br$^-$ anion in both structures interacts with other receptor molecules through C–H HB and ion-pairing to balance the two positive charges associated with the receptor. The significant reduction (up to 0.158 Å) in HB–XB (**G2XBme^{2+}·2Br$^-$**) distance over the non-HB–XB (**G1XBme^{2+}·2Br$^-$**) supports the HB–XB enhancement observed in the computational and solution studies.

Crystals of **G2XB^{2+}** and **G1XBme^{2+}** were also obtained with I$^-$ (Fig. 6) and the structural features parallel the Br$^-$ complexes. Both **G1XBme^{2+}** and **G2XB^{2+}** form bidentate XB interactions with one I$^-$. Again, **G2XB^{2+}** forms intramolecular HBs to both XB iodine donors in **G2XB^{2+}·2I$^-$** with N–H···I distances and angles of 2.94 (13) Å, 168 (8)° and 3.00 (7) Å, 170 (8)°. These HBs preorganize the complex of **G2XB^{2+}·2I$^-$** resulting in pyridinium rings that twist out of coplanarity with the fluoroaniline core by only 2.4 (3) and 2.8 (3)°. In comparison, the pyridinium rings of **G1XBme^{2+}·2I$^-$** deviate from planarity with the core benzene by 14.0 (2) and 14.8 (2)°. Again, the HB–XBs produce closer, stronger XB contacts with the anion. The XB distances and angles in **G2XB^{2+}·2I$^-$** are 3.363 (11) Å, 168.7 (3)° and 3.3865 (11) Å, 176.9 (2)° (R_{II} values are 0.82 and 0.83). The weaker XBs in **G1XBme^{2+}2I$^-$** have distances and angles of 3.5235 (6) Å, 169.82 (19)° and 3.5085 (7) Å, 170.70 (16)° (R_{II} values are 0.87 and 0.86).

Also, the second I$^-$ anion in both systems interacts with other receptor molecules through C–H HB and ion-pairing to balance the two positive charges associated with the receptor. The nearly 0.16 Å reduction in the XB contacts and more planar conformations in **G2XB^{2+}** over **G1XBme^{2+}** support that intramolecular HB–XBs facilitate preorganization and XB enhancement.

A bidentate structure with Cl$^-$ was also obtained for **G1XBme^{2+}** but not **G2XBme^{2+}** (Fig. 7). The XB distances and angles are 3.1530 (9) Å, 171.08 (9)° and 3.3527 (9) Å, 162.19 (9)° (R_{ICl} values of 0.82 and 0.87). The second anion is held above the complex through C–H HB and ion-pairing that help balance the two positive charges associated with the receptor. The pyridinium rings of **G1XBme^{2+}·2Cl$^-$** are twisted out of planarity with the benzene core by 3.83 (11) and 8.33 (11)°. This structure is more planar than the Br$^-$ and I$^-$ structures of **G1XBme^{2+}**. In contrast, the XBs of **G1XBme^{2+}·2Cl$^-$** are not as linear as **G2XB^{2+}** and **G2XBme^{2+}**.

Monodentate XB structures

Crystallization with the OTf$^-$ anion induces monodentate XBing for both **G2XBme^{2+}** and **G1XBme^{2+}**. However, **G2XBme^{2+}·2OTf$^-$**, with intramolecular HBs crystallizes in both the bidentate (Fig. 8a) and monodentate S conformation (Fig. 8b) (≈50/50 disorder). The bidentate conformer of **G2XBme^{2+}·2OTf$^-$** contains one OTf$^-$ molecule in the binding pocket that accepts two XBs to two separate oxygen atoms. The amine HBs to the XB donors with N–H···I distances and angles of 2.9672 (6) Å, 168.1 (2)° and 3.0546 (3) Å, 166.5 (3)°. The bidentate XB distances and angles are 3.195 (10) Å, 172.7 (3)° and 3.280 (9) Å, 148.4 (2)° (R_{IO} values of 0.90 and 0.93).

The monodentate S conformer of **G2XBme^{2+}·2OTf$^-$** provides a unique comparison of two types of XB donors within the same structure, one that accepts an amine HB (HB–XB) and one that does not. The HB–XB donor forms a stronger XB to the OTf$^-$ with a distance and angle of 2.908 (8) Å, 175.91 (18)° (R_{IO} value of 0.82). Whereas the other XB has a distance and angle of 3.089 (6) Å, 168.1 (2)° (R_{IO} value of 0.87). The greater than 0.18 Å reduction in XB distance (between the HB–XB and non-HB–XB donors) is comparable to the Br$^-$ and I$^-$ structures discussed previously.
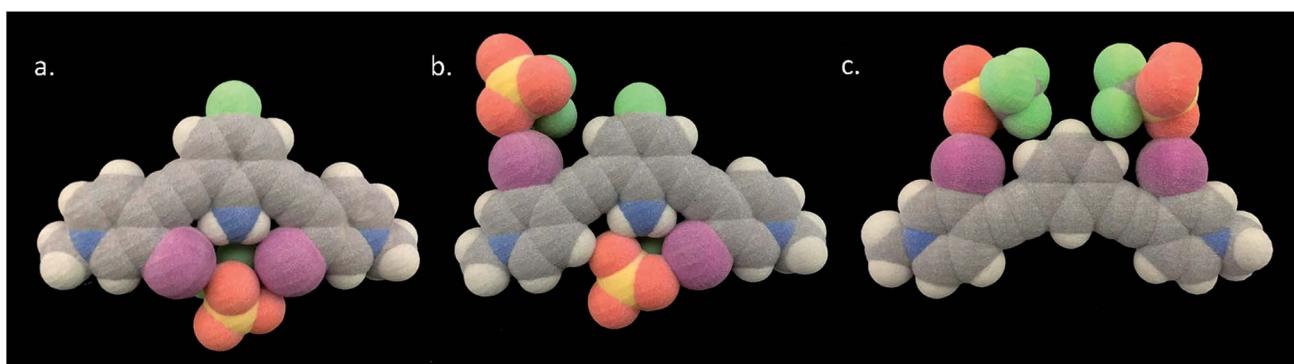

Fig. 8 3D prints generated from the crystal structures (vdW radii) of disordered **G2XBme^{2+}·2OTf$^-$** the bidentate (a) and S conformations (b) and **G1XBme^{2+}·2OTf$^-$** in the W conformation (c).

The crystal of **G1XBme^{2+}·2OTf$^-$**—lacking the preorganizing amine—adopts the W conformation (Fig. 8c). Crystallographic symmetry of this structure dictates a single unique XB contact with a distance and angle of 2.886 (3) Å and 169.28 (10)° (R_{IO} value of 0.82). This contact is shorter than those observed in **G2XBme^{2+}·2OTf$^-$**, likely a result of each OTf$^-$ anion accepting only one XB. Unfortunately, the structural differences prevent a direct comparison of XB strength between **G2XBme^{2+}·2OTf$^-$** and **G1XBme^{2+}·2OTf$^-$**.

The crystals of **G2XBme^{2+}** and **G2XB^{2+}** confirm that intramolecular HB–XBs can preorganize a receptor while simultaneously enhancing the XB. The Br$^-$ and I$^-$ comlexes show a marked reduction in XB distance, signifying an increase in XB strength. Furthermore, **G2XBme^{2+}** and **G2XB^{2+}** are more planar due to intramolecular HB–XB preorganization. The amine limits the monodentate conformation observed in **G2XBme^{2+}·2OTf$^-$**, which further supports preorganization. These crystallographic studies demonstrate the dual function of the intramolecular HB–XB to simultaneously preorganize and strengthen the XB.

Conclusions

In this work we have introduced a polarization-enhanced XB, the intramolecular HB–XB, as a practical strategy to pre-organize halogen containing molecules and augment XB strength. Solution studies of a series of four receptors demonstrated that HB–XBing enhances halide binding by nearly 9-fold over the control receptors. Simultaneous pre-organization and enhancement of the XB was confirmed by gas-phase DFT calculations of single point energies, ESP maps, interaction energies and alkyne conformational analyses. In the solid-state, contracted HB–XB distances with I$^-$ and Br$^-$ and more planar HB–XB receptors supported the gas-phase and solution findings. These results highlight that the intramolecular HB–XB is a new method to both preorganize structure and regulate XB strength.

The unique characteristics of the XB continue to inspire new approaches in chemistry and biochemistry. We hypothesize several benefits of the HB–XB such as: (i) gentle (non-rigid) preorganization, halogens are relatively weak HB acceptors and we envision that molecules employing HB–XBs would enable both preorganization and induced fit binding; (ii) hydrophobicity, the size and lipophilic nature of the halogen will sterically shield intramolecular HBs without drastically increasing the hydrophilicity of the host. These properties will benefit numerous applications including those related to self-assembly, drug development and synthetic ion channels. Studies to understand the factors that influence intramolecular HB–XB strength (*e.g.*, solvent, electron donating/withdrawing effects and HSAB complementarity between HB donor and XB donor) are currently underway in our lab.

Conflicts of interest

There are no conflicts to declare.

Notes and references

§ Preorganization is the notion that it is energetically favorable to arrange binding sites that minimize conformational change upon guest binding. E. V. Anslyn, and D. A. Dougherty, *Modern Physical Organic Chemistry*, University Science, Sausalito, CA, 2006.

¶ The XB is complex in nature with multiple contributions from electrostatics, charge-transfer and polar flattening. Specifically, electrostatic investigations do not always offer a complete description of the XB.

‖ Traditionally, XB strength is strengthened by introducing electron withdrawing groups and/or exchanging the halogen with a more polarizable halogen.

** Beer and coworkers highlight another example of preorganization by metal coordination (Mole *et al. J. Organomet. Chem.* 2015, **792**, 206–210).

†† Elegant macrocycles and foldamers have employed fluorine and chlorine as HB acceptors to encourage higher order structures. See ref. 42. However, HBing is clearly the dominate force in facilitating function. As expected, XBing is not mentioned as contributing to the function of these systems as fluorine and chlorine are very poor XB donors when compared to iodine and bromine XB donors.

‡‡ Only the more capable XB donors of iodine and bromine are considered here. In another report, Zhu *et al.* provide solution data demonstrating intramolecular HBs can be formed with fluorinated, chlorinated and brominated aromatic amides. However, these would not be considered good XB donors and XBing was not mentioned. Zhu *et al. Cryst. Growth Des.* 2008, **8**, 1294–1300.

§§ **G2XB** and **G2HB** were investigated by IR spectroscopy to lend support to intramolecular hydrogen bonding, however no conclusive shifting was observed. The effects of weak hydrogen bonds are not as straightforward as strong hydrogen bonds. Specifically, simple systems can produce spectral complexity which can prevent proper interpretation. However, lack of chemical shift does not indicate absence of hydrogen bonding. More can be found on this topic in Baker *et al. J. Am. Chem. Soc.* 1958, **80**, 5358; A. W. Baker, *J. Am. Chem. Soc.* 1958, **80**, 3598; G. R. Desiraju and T. Steiner, *The Weak Hydrogen Bond in Structural Chemistry and Biology*, Oxford University Press, Oxford, 1999.

¶¶ **G2HB** exhibits an upfield shift due to the relative acidity of the amine protons. The relatively weak iodine HB acceptors could contribute to the relatively small differences observed between **G2XB** and **G2HB**.

‖‖ The B3LYP functional does not accurately estimate the XB. However, this functional correctly estimates the HB interaction to the Lewis base sites of the XB donor.

**** It is known that the electrostatic potential of a molecule is influenced by neighboring atoms, and a decrease in σ-hole electron density does not necessarily correlate with a more positive electrostatic potential. However, our collective findings indicate that the electron density and the electrostatic potential for this system tract. Further discussion on ESP in σ-hole interactions is found here: P. Politzer, and J. Murray, *Crystals*, 2017, 7, 212, DOI: 10.3390/cryst7070212.

††† A CSD search of HBs to organic iodine atoms was compared to **G2XBme^{2+}·2Br$^-$**, **G2XBme^{2+}·2I$^-$**, and **G2XBme^{2+}·2OTf$^-$**. See ESI† for details.

1 D. J. Cram, *Angew. Chem., Int. Ed.*, 1986, **25**, 1039–1057.
2 J.-M. Lehn, *Proc. Natl. Acad. Sci. U. S. A.*, 2002, **99**, 4763–4768.
3 J. B. Wittenberg and L. Isaacs, in *Supramolecular Chemistry: From Molecules to Nanomaterials*, ed. P. A. Gale and J. W.

Steed, John Wiley & Sons Ltd, Chichester, UK, 2012, vol. 1, ch. 3, pp. 25–44.

4 C. Lad, N. H. Williams and R. Wolfenden, *Proc. Natl. Acad. Sci. U. S. A.*, 2003, **100**, 5607–5610.

5 M. H. M. Olsson, W. W. Parson and A. Warshel, *Chem. Rev.*, 2006, **106**, 1737–1756.

6 A. Gutteridge and J. Thornton, *J. Mol. Biol.*, 2005, **346**, 21–28.

7 A. Warshel, P. K. Sharma, M. Kato, Y. Xiang, H. Liu and M. H. M. Olsson, *Chem. Rev.*, 2006, **106**, 3210–3235.

8 P. T. R. Rajagopalan and S. J. Benkovic, *Chem. Rec.*, 2002, **2**, 24–36.

9 A. Pohorille, M. A. Wilson and G. Shannon, *Life*, 2017, **7**, 23.

10 D. J. Cram and G. M. Lein, *J. Am. Chem. Soc.*, 1985, **107**, 3657–3668.

11 D. J. Cram, T. Kaneda, R. C. Helgeson, B. Brown, C. B. Knobler, E. Maverick and K. N. Trueblood, *J. Am. Chem. Soc.*, 1985, **107**, 3645–3657.

12 J.-M. Lehn, *Angew. Chem., Int. Ed.*, 1990, **29**, 1304–1319.

13 J.-M. Lehn, *Science*, 2002, **295**, 2400–2403.

14 J. J. Christensen, D. J. Eatough and R. M. Izatt, *Chem. Rev.*, 1973, 351–384.

15 A. Caballero, N. G. White and P. D. Beer, *Angew. Chem., Int. Ed.*, 2011, **50**, 1845–1848.

16 K. Choi and A. D. Hamilton, *Coord. Chem. Rev.*, 2003, **240**, 101–110.

17 B. Hasenknopf, J.-M. Lehn, B. O. Kneisel, G. Baum and D. Fenske, *Angew. Chem., Int. Ed.*, 1996, **35**, 1838–1840.

18 T. J. Wedge and M. F. Hawthorne, *Coord. Chem. Rev.*, 2003, **240**, 111–128.

19 M. S. Vickers and P. D. Beer, *Chem. Soc. Rev.*, 2007, **36**, 211–225.

20 M. J. Langton, S. W. Robinson, I. Marques, V. Félix and P. D. Beer, *Nat. Chem.*, 2014, **6**, 1039–1043.

21 M. R. Sambrook, P. D. Beer, J. A. Wisner, R. L. Paul and A. R. Cowley, *J. Am. Chem. Soc.*, 2004, **126**, 15364–15365.

22 M. A. Kline, X. Wei, I. J. Horner, R. Liu, S. Chen, S. Chen, K. Y. Yung, K. Yamato, Z. Cai, F. V. Bright, X. C. Zeng and B. Gong, *Chem. Sci.*, 2015, **6**, 152–157.

23 P. V. Santacroce, J. T. Davis, M. E. Light, P. A. Gale, J. C. Iglesias-Sánchez, P. Prados and R. Quesada, *J. Am. Chem. Soc.*, 2007, **129**, 1886–1887.

24 K. P. McDonald, B. Qiao, E. B. Twum, S. Lee, P. J. Gamache, C.-H. Chen, Y. Yi and A. H. Flood, *Chem. Commun.*, 2014, **50**, 13285–13288.

25 S. Lee, Y. Hua, H. Park and A. H. Flood, *Org. Lett.*, 2010, **12**, 2100–2102.

26 J. Shang, W. Si, W. Zhao, Y. Che, J. L. Hou and H. Jiang, *Org. Lett.*, 2014, **16**, 4008–4011.

27 D. C. Sherrington and K. A. Taskinen, *Chem. Soc. Rev.*, 2001, **30**, 83–93.

28 S. H. Jungbauer, S. Schindler, E. Herdtweck, S. Keller and S. M. Huber, *Chem. - Eur. J.*, 2015, **21**, 13625–13636.

29 S. H. Jungbauer and S. M. Huber, *J. Am. Chem. Soc.*, 2015, **137**, 12110–12120.

30 S. K. Kim and J. L. Sessler, *Chem. Soc. Rev.*, 2010, **39**, 3784.

31 A. J. McConnell and P. D. Beer, *Angew. Chem., Int. Ed.*, 2012, **51**, 5052–5061.

32 J. Fernández-Lodeiro, C. Núñez, C. S. de Castro, E. Bértolo, J. S. Seixas de Melo, J. L. Capelo and C. Lodeiro, *Inorg. Chem.*, 2013, **52**, 121–129.

33 P. Molina, F. Zapata and A. Caballero, *Chem. Rev.*, 2017, **117**, 9907–9972.

34 Z. Xu, N. J. Singh, J. Lim, J. Pan, H. N. Kim, S. Park, K. S. Kim and J. Yoon, *J. Am. Chem. Soc.*, 2009, **131**, 15528–15533.

35 B. Gong, Y. Yan, H. Zeng, E. Skrzypczak-Jankunn, Y. W. Kim, J. Zhu and H. Ickes, *J. Am. Chem. Soc.*, 1999, **121**, 5607–5608.

36 X. Yang, A. L. Brown, M. Furukawa, S. Li, W. E. Gardinier, E. J. Bukowski, F. V Bright, C. Zheng, X. C. Zeng and B. Gong, *Chem. Commun.*, 2003, 56–57.

37 S. M. Biros and J. Rebek Jr., *Chem. Soc. Rev.*, 2007, **36**, 93–104.

38 B. W. Purse and J. Rebek, *Proc. Natl. Acad. Sci. U. S. A.*, 2005, **102**, 10777–10782.

39 D. M. Rudkevich, G. Hilmersson and J. Rebek, *J. Am. Chem. Soc.*, 1997, **119**, 9911–9912.

40 A. Vargas Jentzsch, A. Hennig, J. Mareda and S. Matile, *Acc. Chem. Res.*, 2013, **46**, 2791–2800.

41 Y. Hamuro, S. J. Geib and A. D. Hamilton, *Angew. Chem., Int. Ed.*, 1994, **33**, 446–448.

42 D. W. Zhang, X. Zhao, J. L. Hou and Z. T. Li, *Chem. Rev.*, 2012, **112**, 5271–5316.

43 G. R. Desiraju, P. S. Ho, L. Kloo, A. C. Legon, R. Marquardt, P. Metrangolo, P. Politzer, G. Resnati and K. Rissanen, *Pure Appl. Chem.*, 2013, **85**, 1711–1713.

44 A. Brown and P. D. Beer, *Chem. Commun.*, 2016, **52**, 8645–8658.

45 G. Cavallo, P. Metrangolo, R. Milani, T. Pilati, A. Priimagi, G. Resnati and G. Terraneo, *Chem. Rev.*, 2016, **116**, 2478–2601.

46 R. Tepper and U. S. Schubert, *Angew. Chem., Int. Ed.*, 2018, **57**, 6004.

47 P. Auffinger, F. A. Hays, E. Westhof and P. S. Ho, *Proc. Natl. Acad. Sci. U. S. A.*, 2004, **101**, 16789–16794.

48 R. K. Rowe and P. S. Ho, *Acta Crystallogr., Sect. B: Struct. Sci., Cryst. Eng. Mater.*, 2017, **73**, 255–264.

49 T. Clark, M. Hennemann, J. S. Murray and P. Politzer, *J. Mol. Model.*, 2007, **13**, 291–296.

50 N. Busschaert, C. Caltagirone, W. Van Rossom and P. A. Gale, *Chem. Rev.*, 2015, **115**, 8038–8155.

51 F. Kniep, S. H. Jungbauer, Q. Zhang, S. M. Walter, S. Schindler, I. Schnapperelle, E. Herdtweck and S. M. Huber, *Angew. Chem., Int. Ed.*, 2013, **52**, 7028–7032.

52 S. M. Walter, F. Kniep, E. Herdtweck and S. M. Huber, *Angew. Chem., Int. Ed.*, 2011, **50**, 7187–7191.

53 P. Metrangolo and G. Resnati, *Chem.–Eur. J.*, 2001, **7**, 2511–2519.

54 P. Metrangolo, T. Pilati, G. Terraneo, S. Biella and G. Resnati, *CrystEngComm*, 2009, **11**, 1187.

55 G. Cavallo, P. Metrangolo, T. Pilati, G. Resnati, M. Sansotera and G. Terraneo, *Chem. Soc. Rev.*, 2010, **39**, 3772.

56 O. Dumele, B. Schreib, U. Warzok, N. Trapp, C. A. Schalley and F. Diederich, *Angew. Chem., Int. Ed.*, 2017, **56**, 1152–1157.

57 O. Dumele, N. Trapp and F. Diederich, *Angew. Chem., Int. Ed.*, 2015, **54**, 12339–12344.

58 N. K. Beyeh, F. Pan and K. Rissanen, *Angew. Chem.*, 2015, **127**, 7411–7415.

59 C. J. Massena, N. B. Wageling, D. A. Decato, E. Martin Rodriguez, A. M. Rose and O. B. Berryman, *Angew. Chem., Int. Ed.*, 2016, **55**, 12398–12402.

60 F. Zapata, A. Caballero, P. Molina, I. Alkorta and J. Elguero, *J. Org. Chem.*, 2014, **79**, 6959–6969.

61 R. Tepper, B. Schulze, H. Görls, P. Bellstedt, M. Jäger and U. S. Schubert, *Org. Lett.*, 2015, **17**, 5740–5743.

62 A. Caballero, F. Zapata, N. G. White, P. J. Costa, V. Félix and P. D. Beer, *Angew. Chem., Int. Ed.*, 2012, **51**, 1876–1880.

63 F. Zapata, A. Caballero, N. G. White, T. D. W. Claridge, P. J. Costa, V. Félix and P. D. Beer, *J. Am. Chem. Soc.*, 2012, **134**, 11533–11541.

64 T. Steiner, *Angew. Chem., Int. Ed.*, 2002, **41**, 48–76.

65 G. A. Jeffrey and W. Saenger, *Hydrogen Bonding in Biological Structures*, Springer Berlin Heidelberg, Berlin, Heidelberg, 1991.

66 C. B. Aakeröy, C. L. Spartz, S. Dembowski, S. Dwyre and J. Desper, *IUCrJ*, 2015, **2**, 498–510.

67 C. B. Aakeröy, P. D. Chopade and J. Desper, *Cryst. Growth Des.*, 2011, **11**, 5333–5336.

68 P. Politzer, J. S. Murray and P. Lane, *Int. J. Quantum Chem.*, 2007, **107**, 3046–3052.

69 A. R. Voth, P. Khuu, K. Oishi and P. S. Ho, *Nat. Chem.*, 2009, **1**, 74–79.

70 M. G. Chudzinski, C. A. McClary and M. S. Taylor, *J. Am. Chem. Soc.*, 2011, **133**, 10559–10567.

71 B. R. Mullaney, A. L. Thompson and P. D. Beer, *Angew. Chem., Int. Ed.*, 2014, **53**, 11458–11462.

72 C. B. Aakeröy, M. Fasulo, N. Schultheiss, J. Desper and C. Moore, *J. Am. Chem. Soc.*, 2007, **129**, 13772–13773.

73 A. Takemura, L. J. McAllister, S. Hart, N. E. Pridmore, P. B. Karadakov, A. C. Whitwood and D. W. Bruce, *Chem.–Eur. J.*, 2014, **20**, 6721–6732.

74 V. Vasylyeva, S. K. Nayak, G. Terraneo, G. Cavallo, P. Metrangolo and G. Resnati, *CrystEngComm*, 2014, **16**, 8102–8105.

75 P. Zhou, J. Lv, J. Zou, F. Tian and Z. Shang, *J. Struct. Biol.*, 2010, **169**, 172–182.

76 Y. Lu, Y. Wang, Z. Xu, X. Yan, X. Luo, H. Jiang and W. Zhu, *J. Phys. Chem. B*, 2009, **113**, 12615–12621.

77 Q. Zhao, D. Feng and J. Hao, *J. Mol. Model.*, 2011, **17**, 2817–2823.

78 P.-P. Zhou, W.-Y. Qiu, S. Liu and N.-Z. Jin, *Phys. Chem. Chem. Phys.*, 2011, **13**, 7408.

79 A. Kovács and Z. Varga, *Coord. Chem. Rev.*, 2006, **250**, 710–727.

80 M. Domagała and M. Palusiak, *Comput. Theor. Chem.*, 2014, **1027**, 173–178.

81 M. Domagała, A. Lutyńska and M. Palusiak, *Int. J. Quantum Chem.*, 2017, **117**, e25348.

82 L. Albrecht, R. J. Boyd, O. Mó and M. Yáñez, *J. Phys. Chem. A*, 2014, **118**, 4205–4213.

83 A. S. Mahadevi and G. N. Sastry, *Chem. Rev.*, 2016, **116**, 2775–2825.

84 M. Solimannejad, M. Malekani and I. Alkorta, *Mol. Phys.*, 2011, **109**, 1641–1648.

85 S. A. C. McDowell and H. K. Yarde, *Phys. Chem. Chem. Phys.*, 2012, **14**, 6883.

86 H. Sun, C. Navarro and C. A. Hunter, *Org. Biomol. Chem.*, 2015, **13**, 4981–4992.

87 F. Y. Lin and A. D. Mackerell, *J. Phys. Chem. B*, 2017, **121**, 6813–6821.

88 C. J. Massena, A. M. S. Riel, G. F. Neuhaus, D. a. Decato and O. B. Berryman, *Chem. Commun.*, 2015, **51**, 1417–1420.

89 A. M. S. Riel, M. J. Jessop, D. A. Decato, C. J. Massena, V. R. Nascimento and O. B. Berryman, *Acta Crystallogr., Sect. B: Struct. Sci., Cryst. Eng. Mater.*, 2017, **73**, 203–209.

90 K. Sonogashira, Y. Tohda and N. Hagihara, *Tetrahedron Lett.*, 1975, **16**, 4467–4470.

91 D. L. Reger, T. D. Wright, C. A. Little, J. J. S. Lamba and M. D. Smith, *Inorg. Chem.*, 2001, **40**, 3810–3814.

92 C. Frassineti, S. Ghelli, P. Gans, A. Sabatini, M. S. Moruzzi and A. Vacca, *Anal. Biochem.*, 1995, **231**, 374–382.

93 M. Cametti, K. Raatikainen, P. Metrangolo, T. Pilati, G. Terraneo and G. Resnati, *Org. Biomol. Chem.*, 2012, **10**, 1329.

94 C. C. Robertson, R. N. Perutz, L. Brammer and C. A. Hunter, *Chem. Sci.*, 2014, **5**, 4179–4183.

95 R. D. Parra, H. Zeng, J. Zhu, C. Zheng, X. C. Zeng and B. Gong, *Chem.–Eur. J.*, 2001, **7**, 4352–4357.

96 E. Peris, J. C. J. Lee, J. R. Rambo, O. Eisenstein and R. H. Crabtree, *J. Am. Chem. Soc.*, 1995, **117**, 3485–3491.

97 Y.-Y. Zhu, H.-P. Yi, C. Li, X.-K. Jiang and Z.-T. Li, *Cryst. Growth Des.*, 2008, **8**, 1294–1300.

98 L. R. Steffel, T. J. Cashman, M. H. Reutershan and B. R. Linton, *J. Am. Chem. Soc.*, 2007, **129**, 12956–12957.

99 P. Froimowicz, K. Zhang and H. Ishida, *Chem.–Eur. J.*, 2016, **22**, 2691–2707.

100 M. J. Frisch, G. W. Trucks, H. B. Schlegel, G. E. Scuseria, M. A. Robb, J. R. Cheeseman, G. Scalmani, V. Barone, B. Mennucci, G. A. Petersson, H. Nakatsuji, M. Caricato, X. Li, H. P. Hratchian, A. F. Izmaylov, J. Bloino, G. Zheng, J. L. Sonnenberg, M. Hada, M. Ehara, K. Toyota, R. Fukuda, J. Hasegawa, M. Ishida, T. Nakajima, Y. Honda, O. Kitao, H. Nakai, T. Vreven, J. A. Montgomery Jr, J. E. Peralta, F. Ogliaro, M. Bearpark, J. J. Heyd, E. Brothers, K. N. Kudin, V. N. Staroverov, R. Kobayashi, J. Normand, K. Raghavachari, A. Rendell, J. C. Burant, S. S. Iyengar, J. Tomasi, M. Cossi, N. Rega, N. J. Millam, M. Klene, J. E. Knox, J. B. Cross, V. Bakken, C. Adamo, J. Jaramillo, R. Gomperts, R. E. Stratmann, O. Yazyev, A. J. Austin, R. Cammi, C. Pomelli, J. W. Ochterski, R. L. Martin, K. Morokuma, V. G. Zakrzewski, G. A. Voth, P. Salvador, J. J. Dannenberg, S. Dapprich, A. D. Daniels, O. Farkas, J. B. Foresman, J. V. Ortiz, J. Cioslowski and D. J. Fox, *Gaussian 09, Revision B.01*, Gaussian, Inc., Wallingford CT, 2009.

101 J. E. Del Bene, *J. Phys. Chem.*, 1993, **97**, 107–110.

102 M. G. Chudzinski and M. S. Taylor, *J. Org. Chem.*, 2012, 77, 3483–3491.

103 K. L. Schuchardt, B. T. Didier, T. Elsethagen, L. Sun, V. Gurumoorthi, J. Chase, J. Li and T. L. Windus, *J. Chem. Inf. Model.*, 2007, **47**, 1045–1052.